Collision-induced absorption and electric quadrupole transitions of N2 by OF-CEAS near 4.0 μm and CRDS near 2.1 μm

L. Richard, D. Mondelain, S. Kassi, I. Ventrillard, D. Romanini, A. Campargue

Collision-induced absorption and electric quadrupole transitions of N_2 by OF-CEAS near 4.0 μm and CRDS near 2.1μm

L. Richard, D. Mondelain, S. Kassi, I. Ventrillard, D. Romanini and A. Campargue *

[1] Univ. Grenoble Alpes, CNRS, LIPhy, 38000 Grenoble, France

Key words: Nitrogen; N_2; dinitrogen; Collision Induced Absorption; CIA; electric quadrupolar transitions, CRDS; OF-CEAS

Number of Pages: 20
Number of Figures: 8
Number of Tables: 3

**Corresponding author*: Alain Campargue (Alain.Campargue@univ-grenoble-alpes.fr)

Abstract

Highly sensitive cavity enhanced laser techniques are used for accurate measurements of the absorption of dinitrogen (N_2) at two spectral points of the fundamental and first overtone bands. Spectra of pure N_2 and of N_2/O_2 mixture were recorded near 2492 and 4720 cm^{-1} by Optical Feedback Cavity Enhanced Absorption Spectroscopy (OF-CEAS) and Cavity Ring Down Spectroscopy (CRDS), respectively. The noise level of the OF-CEAS and CRDS spectra corresponds to a minimum detectable absorption, α_{min}, of about 10^{-9} and 10^{-11} cm^{-1}, respectively. Measurements involve both the N_2 collision-induced absorption (CIA) bands and the very weak 2–0 *S*(10) and *S*(11) electric quadrupolar transitions. Accurate CIA binary coefficients, $B_{N_2-N_2}$ and $B_{N_2-O_2}$, are derived from the pressure-squared dependence of the baseline level of the spectra recorded at pressures below 1 atm. These CIA values are compared to previous determinations from high pressure spectra (up to 90 atm) and to recent classical molecular dynamics simulations (CMDS). An overall good agreement is obtained although a significant deviation is observed for the first overtone CIA near 4720 cm^{-1}. The line position and intensity (on the order of a few 10^{-30} cm/molecule) of the 2–0 *S*(10) and *S*(11) electric quadrupolar transitions are determined experimentally for the first time and compared to theoretical values provided in the HITRAN2016 database.

1. Introduction

The absorption of light by dinitrogen, N_2, is very weak. Being a homonuclear diatomic molecule, $^{14}N_2$ has no dipole-allowed vibrational bands and its rovibrational infrared spectrum consists of extremely weak quadrupolar bands formed of rotational lines following the $\Delta J = 0, \pm 2$ selection rules (where J is the rotational quantum number) [1-6]. As a consequence of their weakness, the detection of N_2 quadrupole transitions by absorption is difficult and mostly limited to the 1-0 fundamental band centered at 2250 cm^{-1} [1-4]. This band, firstly reported by Goldman et al. [1] and Camy-Peyret et al. [2] from long path atmospheric spectra, is now routinely observed and modeled in the atmospheric spectra recorded by Fourier Transform Spectroscopy (FTS) in the frame of the Total Carbon Column Observing Network (TCCON) [7].

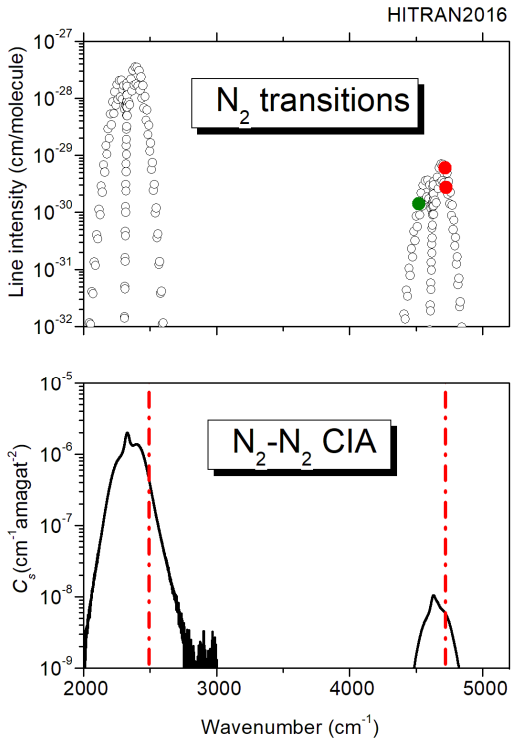

Fig. 1

Overview of the N_2 room temperature absorption between 2000 and 5000 cm^{-1} as provided by the HITRAN2016 database [9,10].

Upper panel: Quadrupolar electric transitions of the fundamental and first overtone bands of $^{14}N_2$ [9]. The 2–0 $S(10)$ and $S(11)$ electric quadrupole transitions measured in this work are highlighted (red circles) together with the 2–0 $O(14)$ transitions measured by CRDS in Ref. [11] (green circle).

Lower panel: Collision Induced Absorption bands as provided in the HITRAN database [10]. The HITRAN data are derived from the experimental results by Baranov and Lafferty for the fundamental band [12] and from results of classical molecular dynamics simulations (CMDS) for the first overtone [13]. The dashed lines indicate the spectral points of the measurements reported in this work.

In fact, in the atmosphere of Earth and of other bodies in the Solar System (e.g. Titan or Triton), most of the N_2 absorption is not due to quadrupolar bands but to the collision-induced absorption (CIA) bands. The CIA bands result from the transient dipole moment induced by collisions

of N_2 molecules with N_2 (and O_2, in our atmosphere) and thus scale as the product of the densities of N_2 and of the collisional partner [8]. **Fig. 1** shows an overview of the fundamental and first overtone quadrupolar bands of N_2 together with their corresponding N_2-N_2 CIA bands, as provided by the HITRAN spectroscopic database [9,10].

The laboratory measurement of the very weak nitrogen CIA bands is made difficult because of the weakness of the signal to be detected as a small and spectrally broad depletion of the light intensity transmitted through an absorption cell containing the gas The maximum of absorption for the fundamental and first overtone CIA are on the order of 10^{-6} and 10^{-8} $cm^{-1}/amagat^2$, respectively. A few previous works have been devoted to the N_2-N_2 CIA bands [12,14-17] (see **Table 1**). Spectra were recorded with grating spectrographs or by FTS associated with high pressure multipass cells. Pressure values up to 90 atm [14] were used to enhance the CIA signal (proportional to the pressure-squared). In support of planetary studies, the temperature dependence of the CIAs was also investigated at 97.5 K [17].

In the present contribution, we use highly sensitive laser techniques to measure N_2-N_2 CIA around two spectral points of the fundamental and first overtone bands. The measurement points located near 2492 and 4720 cm^{-1} are indicated on the bottom of **Fig. 1**. The used laser absorption techniques, namely, Optical Feedback Cavity Enhanced Absorption Spectroscopy (OF-CEAS) and Cavity Ring Down Spectroscopy (CRDS), are based on the coupling of laser sources and high finesse optical cavities containing the gas. Although much more limited than FTS in terms of spectral coverage, these techniques are inherently much more sensitive. Our recent accurate characterization of the water vapor absorption continuum by OF-CEAS and CRDS in the 4.0, 2.3, 1.6 and 1.25 µm windows [18-21] and of the O_2 CIA near 1.27 µm [22], have shown that the performances in terms of sensitivity and spectra baseline stability make these techniques ideal to study weak broad band continua. In the following, the first measurements of the N_2 CIA at sub-atmospheric pressures are presented. In the two next sections, the spectra acquisition, the continuum retrieval and a comparison to previous experimental and theoretical results are presented for each of the two spectral points. In Section 4, the detection of the 2–0 *S*(10) and *S*(11) electric quadrupole transitions is reported and the derived line parameters are compared to the values provided by the HITRAN database.

Table 1.
Review of the measurements of the 1-0 and 2-0 CIA bands of N_2 and corresponding experimental conditions and techniques.

Band	Ref	Technique	Pathlength (m)	Pressure (atm)	*T* (K)
1-0	Shapiro and Gush, 1966 [14]	grating	40	4-18.4	room
	Menoux et al. 1993 [15]	grating	8-120	10-90	193-300
	Lafferty et al. 1996 [16]	FTS	84.05	up to 8	230-300
	Baranov et al. 2005 [12]	FTS	84.05 or 116.05	3.5-8	300-360
	This work (2491 cm^{-1})	OF-CEAS	NR[a]	0-1	295.8 and 315.5
2-0	Shapiro and Gush, 1966 [14]	Grating	80	45-90	room
	Mc Kellar, 1989 [17]	FTS	154	3.12 (i.e. 9.3 amagats)	97.5
	This work (4715-4725 cm^{-1})	CRDS	NR[a]	0.66 and 0.99	297.1 (pure N_2)
				0.99	299.3 (N_2-O_2)

[a] NR:not relevant

2. OF-CEAS of the CIA fundamental band at 2491 cm^{-1}

OF-CEAS is a quantitative and highly sensitive laser absorption technique, alternative to CRDS, routinely applied to trace gas measurements [23,24]. OF-CEAS has specific advantages which make it particularly suitable for the measurement of absorption continua. OF-CEAS exploits optical feedback toward the diode laser source selectively produced only at cavity resonances allowing optimized cavity injection by the laser radiation. This is possible thanks to the adopted V-geometry of the high-finesse optical cavity. OF-CEAS is able to generate several spectral scans per second of a narrow spectral region (~1 cm^{-1}). The acquired spectra have an intrinsically linear frequency scale with equally spaced spectral points separated by the cavity Free Spectral Range $FSR=c/2nL$, where c is the speed of light, L the effective cavity length, and n the refractive index of the intra-cavity sample.

The OF-CEAS setup used in this work is similar to that used for water vapor self-continuum measurements [18,20]. The reader is referred to Ref. [18] (in particular, its Fig. 1) for a detailed description of the experimental setup. Here, an Interband Cascade Laser (ICL) emitting around 2491 cm^{-1}, designed by Nanoplus GmbH, is used as the light source. The V-shaped cavity with 6 mm apex diameter cavity is made in a thick stainless steel block drilled from side to side. Each arm of the V-cavity has a length of about 399.6+/-0.4 mm resulting in an effective length of ~800 mm and a FSR= 187.56+/-0.10 MHz. At the laser wavelength, the reflectivity of the cavity mirrors (from LohnStar Optics) is 99.981 %, as deduced from a ring-down time of 6.95 µs measured with evacuated cavity (filled with Ar). Scans over ~1.5 cm^{-1} (~45 GHz) were produced by modulation of the laser current. The duration of one spectral scan corresponding to about 240 cavity modes (FSR) was about 200 ms. By using heating tapes along the cavity and platinum thermistors, the cavity temperature can be controlled between room temperature and about 325 K. Two series of measurements were performed at 295.8 and 315.5 K (22.7°C and 42.4 °C, respectively).

Let us recall that in OF-CEAS, the transmission spectra is converted to loss rate spectra from a measurement of the ring down time (τ) at the last mode of the laser scan [24]. In order to average the scan-to-scan fluctuation of the τ values, an averaged value was determined with an accuracy of 0.2 % from about 800 measurements at fixed pressure value.

A series of about 15000 spectra was recorded during a pressure ramp with total duration between 10 and 12 minutes. The N_2 flow was injected inside the cavity through a needle valve. A pressure controller (IQ+Flow, from Bronkhorst) was placed between the cavity's outlet and the pump to generate pressure ramps between 80 and 1000 mbar. The pressure was monitored at the cavity center by a pressure gauge (CPG2500, from Mensor, 0-1000 mbar) with an accuracy better than 0.5 mbar. **Fig. 2** illustrates the increase of the baseline level of the OF-CEAS spectra during pressure ramps recorded at temperature of 295.8 and 315.5 K. A pure pressure-squared dependence is obtained at the two temperatures. As a test of the mechanical stability of the OF-CEAS setup, N_2 was replaced by Ar and spectra were recorded in the same experimental conditions. As shown in **Fig. 2,** no significant variation of the baseline level was obtained with argon up to 1 atm.

If we consider the general case of an N_2/O_2 mixture, total losses, $\alpha_{tot}(\nu,T)$, are the sum of the cavity losses and of the N_2 CIA:

$$\alpha_{tot}(\nu,T)=\alpha_{cav}(\nu,T)+\alpha_{CIA}(\nu,T)=\alpha_{cav}(\nu,T)+B_{N_2-N_2}(\nu,T)\rho_{N_2}^2+B_{N_2-O_2}(\nu,T)\rho_{O_2}\rho_{N_2} \quad (1)$$

Where:

- $\alpha_{cav}(\nu,T)$ corresponds to the losses of the cavity evacuated (or filled with Ar),
- ρ_i are N_2 and O_2 densities (in amagat) proportional to the partial pressure $P_i = \rho_i kT$ where k is the Boltzmann constant,
- $B_{N_2-N_2}$ and $B_{N_2-O_2}$ are binary collision absorption coefficients (or density normalized absorption) in $cm^{-1}amagat^{-2}$.

The above expression omits losses due to Rayleigh scattering which are negligible near 4 µm.

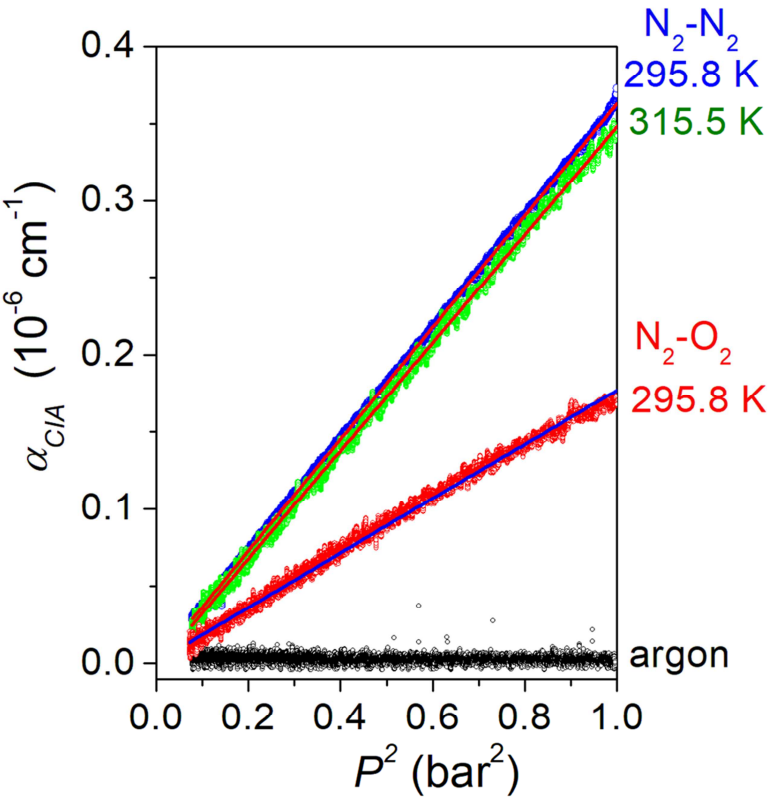

Fig. 2.

Variation of the CIA absorption coefficient near 2491 cm^{-1} as a function of the pressure-squared. Measurements were performed with pure N_2 at 295.8 and 315.5 K and with a 50/50 O_2/N_2 mixture at 295.8 K. The solid lines correspond to the fit of the absorption coefficients by a linear function. Note that the plotted data correspond to the superposition of two or three pressure ramps. The constant term due to the cavity losses, obtained from the fit was subtracted. The measurements performed by using argon instead of N_2 are also plotted and confirm the stability of OF-CEAS baseline against pressure variations up to 1 atm.

In the case of pure N_2, the $B_{N_2-N_2}$ coefficient is readily obtained from the fitted slope of $\alpha_{tot}(\nu,T)$ *versus* P^2 (**Fig. 2**). The corresponding values are given in **Table 2** for the measurements at 22.7°C and 42.4 °C.

Table 2.
Binary coefficients of the 1-0 and 2-0 CIA bands of N_2 derived by OF-CEAS and CRDS near the 2491 and 4720 cm^{-1} spectral points.

Measurement point (cm^{-1})	$B_{N_2-N_2}$ ($cm^{-1}amagat^{-2}$)	$B_{N_2-O_2}$ ($cm^{-1}amagat^{-2}$)	*T(K)*
2491	$4.27(20)\times10^{-7}$	$3.8(8)\times10^{-7}$	295.8(1)
	$4.67(20)\times10^{-7}$		315.5(2)
4715	$7.45(20)\times10^{-9}$		297.1(5)
4725	$6.95(20)\times10^{-9}$		297.1(5)
4715		$5.2(1.4)\times10^{-9}$	299.3(5)
4725		$4.6(1.4)\times10^{-9}$	299.3(5)

Note
Error bars are given in parenthesis in the unit of the last quoted digit

The temperature dependence of the CIA is needed for applications to the Earth and planetary atmospheres. As discussed in Richard et al. [10] and summarized in **Table 1**, Lafferty et al. [16] and Baranov et al. [12] reported FTS measurements of the 1-0 CIA in the 230-300 K and 300-360 K temperature ranges, respectively. **Fig. 3** shows the obtained variation of the $B_{N_2-N_2}$ coefficient at 2491 cm^{-1} together with our values at 295.8 and 315.5 K. Due to the high pressure of the recordings (up to 8 atm), the FTS values were reported with small error bars on the order of 1%. This is significantly better than the uncertainty of our OF-CEAS values which is estimated to be on the order of 5%. The agreement within a few % between the FTS and OF-CEAS results provide a mutual validation of CIA measurements performed in very different pressure conditions.

As part of their analysis of the temperature dependence the 1-0 CIA, Lafferty et al. provided an empirical modeling of their CIA measurements between 230 and 300 K [16]. The wavenumber and temperature dependences of the $B_{N_2-N_2}$ binary coefficient was modeled by using a simple empirical law:

$$B_{N_2-N_2}(\nu,T) = B_0(\nu)\exp[\beta_0(\nu)(1/T_0 - 1/T)] \quad (2)$$

where T_0= 296 K is the reference temperature and B_0 and β_0 are frequency dependent parameters which were provided with a 5 cm^{-1} step between 2125 and 2600 cm^{-1} [16]. The corresponding curves have been included in **Fig. 3** for our measurement point at 2491 cm^{-1} and for the 2300, 2400 and 2450 cm^{-1} wavenumbers. For the experimental values of the $B_{N_2-N_2}$ binary coefficients, we used the values of Lafferty et al. as reproduced by the HITRAN database. The $B_{N_2-N_2}$ values in the 300-390 K range as reported by Baranov et al [12] (and included in the HITRAN database) are also plotted in **Fig. 3** while

195 they were not considered in the fit of B_0 and β_0. On the basis of **Fig. 3**, it appears that the empirical law with the B_0 and β_0 values taken in Table 1 of Ref. [16] does not correspond to the best fit of the experimental data of Lafferty et al. [16] (as provided by the HITRAN database). This is particularly clear at 2300 cm^{-1} and at our spectral point near 2491 cm^{-1}. We do not have any explanation for this situation. As expected the extrapolation of the empirical law to the high temperature range studied by
200 Baranov et al. is not satisfactory. In a recent work devoted to the retrieval of carbon dioxide vertical profiles from solar occultation observations, Sioris et al. [25] reconsidered the original data from Lafferty et al. and found necessary to correct the values of the β_0 parameter. The temperature dependence obtained with these new β_0 values (and B_0 from Ref. [16]) are also plotted in **Fig. 7.** An improvement is noted but the situation is not yet satisfactory. Let us note that better fits can be
205 obtained by using as input data both the measurements of Lafferty et al. and of Baranov et al. covering the 230-390 K temperature range.

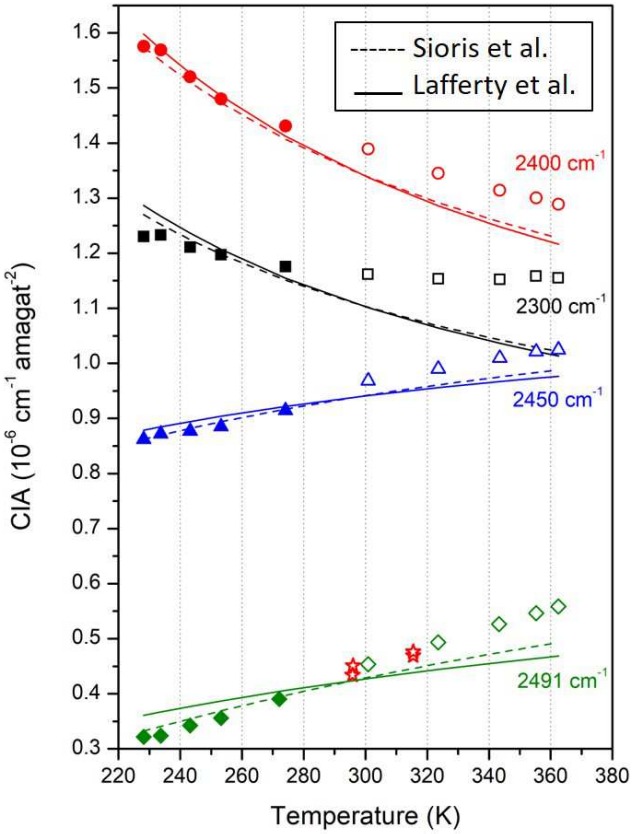

Fig. 3.

Variation of the $B_{N_2-N_2}$ binary coefficient near 2491, 2300, 2400 and 2450 cm^{-1} as a function of
210 the temperature. Literature values from Lafferty et al. [16] below 300 K and Baranov et al. [12] above 300 K (filled and open symbols, respectively) are displayed together with our two measurements points (295.8 and 315.5 K) at 2491 cm^{-1} (red stars). The curves correspond to an empirical law with fitted parameters from Lafferty et al. [16] and Sioris et al. [25] (solid and dashed lines, respectively).

Finally, let us mention that a series of spectra was recorded using a 1:1 mixture of O_2 and N_2. The continuum absorption coefficient varies linearly with the total pressure and is about half than for pure nitrogen (see **Fig. 3**), indicating that the value of the $B_{N_2-O_2}$ binary coefficient is close to that of $B_{N_2-N_2}$ (see Eq. 1). The derived value, $B_{N_2-O_2}$ = 3.8(8)×10^{-7} cm^{-1}amagat^{-2}, leads to a $B_{N_2-O_2}/B_{N_2-N_2}$ ratio of 0.87(18). From their spectra recorded using high pressure samples (N_2 density of 5.5 and 9.5 amagat), Menoux et al. found that the relative efficiency of the colliding partners O_2 and N_2 is practically independent of the wavenumber over the 2150-2500 cm^{-1} region and derived a 0.83(2) value for the ratio of the binary coefficients [15]. Although obtained with larger error bar, our low pressure measurement confirms the results of Ref. [15].

3. CRDS of the CIA first overtone near 4720 cm^{-1}

3.1. Measurements

The CRDS technique is based on the measurement of the decay time (ring down) of the light intensity leaking from a high finesse cavity [24,26,27]. Under vacuum, the ring down time, τ_0, is determined by the reflectivity of the high reflectivity mirrors (*e.g.* R≈1-10^{-5}) and can reach several hundred µs (about 150 µs in the present work). In presence of an intracavity gas, additional losses shorten the ring down time, τ, i.e. increase the loss rate, $1/c\tau$. The absorption coefficient at the wavenumber, ν, is therefore obtained from the variation of the loss rate:

$$\alpha(\nu) = \frac{n}{c\,\tau(\nu)} - \frac{1}{c\,\tau_0(\nu)} \qquad (3)$$

where $1/c\tau_0$ is the loss rate of the empty cavity related to the mirrors reflectivity. The broadband CIA absorption is deduced from a weak increase of the CRDS spectrum baseline. Because an optical misalignment may affect the ring down time, we paid a particular attention to the long term mechanical stability of the assembly under pressure variations and gas handling. Our recent characterizations of the weak water vapor absorption continuum by CRDS in three infrared transparency windows [19-21] have illustrated the performances of the present method with distributed feedback (DFB) laser diodes and an external cavity diode laser (ECDL).

The reader is referred to Refs. [11,28,29] for a description of the CRDS spectrometer dedicated to atmospheric species studies in the 2.3 µm region. A DFB diode laser (8 mW maximum power from Eblana Photonics) is used as light source. Its emission line width is narrowed by applying an optical feedback from an external cavity, as described in [30]. This improves the coupling of the laser to the CRD high finesse cavity and therefore enhances the ring down signal quality. An acousto-optic modulator (AOM), used on first diffraction order, is used to interrupt the injection and initiate the ring-down events. The frequency of the DFB laser diode is continuously monitored with a wavelength meter (model 621-A IR from Bristol, 8 MHz accuracy).

The CRDS cell was filled with either pure Ar (Air Liquide, 99.999% purity), pure N_2 (Air Liquide, 99.9999% purity) or with a reference mixture of O_2+N_2 with an O_2 relative concentration of 20.965±0.022% (1σ) (Air Liquide; O_2+N_2>99.9999%). Pressure was continuously monitored with a 1000 mbar pressure gauge (ATM.1ST from STS, accuracy of ±0.1% of the full scale). The cell temperature was monitored with a TSic 501 sensor (from IST-AG; 0.1 K accuracy) fixed on the cell surface, covered by an external blanket of thermal insulation foam.

Similarly to the OF-CEAS experiments described above for the 1-0 CIA band, our water vapor continuum measurements by CRDS were mostly based on ring-down times measured at fixed optical frequency, during upward and downward pressure ramps [19-21]. This was possible because the amplitude of the pressure ramp was at most 20 mbar but, in the present case, N_2 CIA measurements require a pressure range of 1 atm which may modify the optical alignment of the experimental setup. Therefore, an alternative approach, similar to the one adopted for the CIA of O_2 at 1.27 µm [22], was preferred. The CRDS spectra were recorded over the 4715- 4726 cm^{-1} spectral interval accessible with the DFB laser diode at disposal. The duration of spectra recording being limited to a few minutes, desorption of water from the CRDS cell is limited and spectra could be acquired in static regime at 500, 700 and 750 Torr for pure N_2 and at 750 Torr for the N_2-O_2 mixture. To obtain the baseline and to minimize possible changes of mirrors alignment, spectra were also recorded with argon at the same pressures. For each pressure step the same sequence was adopted: recordings of two N_2 spectra followed by two argon spectra and then again by two N_2 spectra. Between the N_2 and argon spectra the cavity was evacuated. The four N_2 spectra series allowed assessing the baseline stability over time and pumping/filling cycle.

An overview of the N_2 recordings is presented in **Fig. 4.** together with the corresponding Ar recordings. The spectra at pressures of 500 and 750 Torr, shown in **Fig. 4,** reveal a quasi-doubling of the continuum amplitude. Due to relatively strong water vapor transitions in the region (intensities on the order of 10^{-24} cm/molecule), a number of absorption lines are detected in the spectra. The water vapor relative concentration was estimated to be around 25 ppm and 80 ppm in the N_2 spectra and Ar spectra, respectively. Note the smaller pressure broadening of the water lines in Ar compared to N_2.

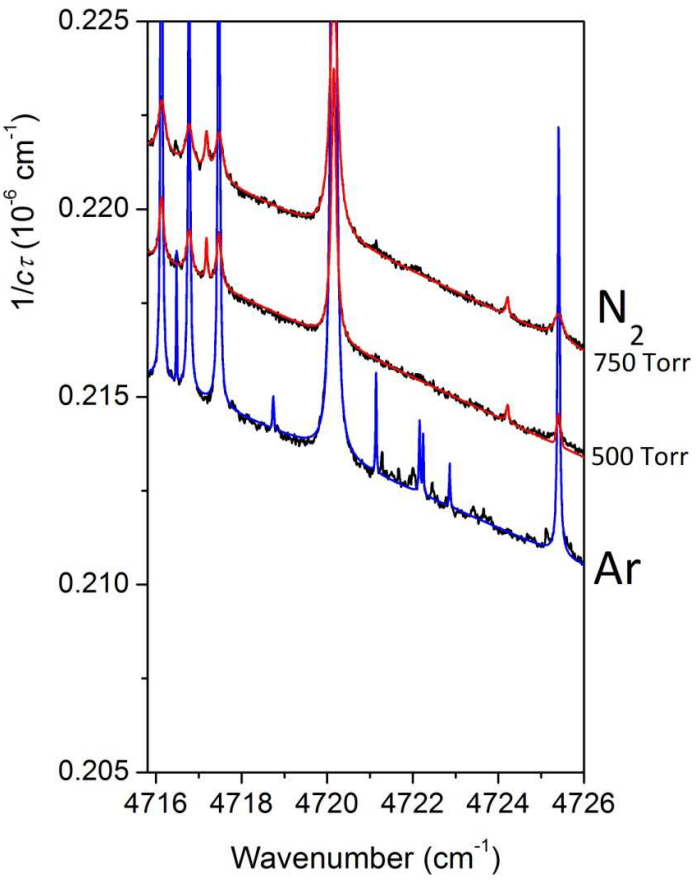

Fig. 4.

Frequency dependence of the loss rates measured by CRDS between 4716 and 4726 cm^{-1} for pure N_2 at 500 and 750 Torr and argon (at 500 Torr). Absorption lines due to water vapor present as an impurity at the 25 ppm and 80 ppm level for N_2 and Ar, respectively, are observed. The solid curves (red and blue for N_2 and Ar, respectively) correspond to the fit of the water line contribution which was subtracted to get the spectra baseline.

To obtain the spectra baseline, the contribution of the water vapor lines was first reproduced using a multiline fitting program and a Voigt function for the line profile. After subtraction of the lines contribution, small losses due to the Rayleigh scattering were considered. Rayleigh scattering cross-sections of Ar and N_2 are close [31] leading to a difference (proportional to pressure) on the order of 6.8×10^{-11} cm^{-1} at 750 Torr. This small effect –the CIA amplitude at 700 Torr is about 7×10^{-9} cm^{-1}– was taken into account in the subtraction of the Ar baselines from the N_2 baselines at the same pressure. The resulting difference is the CIA absorption coefficient, $\alpha_{CIA}(\nu,T)=B_{N_2-N_2}(\nu,T)\rho_{N_2}^2$. The $B_{N_2-N_2}$ binary coefficients derived from the 700 and 750 Torr spectra are presented on **Fig. 5.** Their excellent coincidence (within about 1 %) reflects the pressure-squared dependence of the CIA absorption coefficient. We give in **Table 2**, the $B_{N_2-N_2}$ values recommended at 4715 and 4725 cm^{-1} as obtained from a linear fit of the measured values over the 4715.55- 4726.09 cm^{-1} interval. In our case the main uncertainty for the $B_{N_2-N_2}$ binary coefficients is due to the baseline stability of the spectra which is

estimated to be on the order of 8×10^{-11} cm^{-1}. Uncertainty on density, related to errors on temperature and pressure determinations, can be neglected. We estimate the error bar on the $B_{N_2-N_2}$ values included in **Table 2** to be ~3 %.

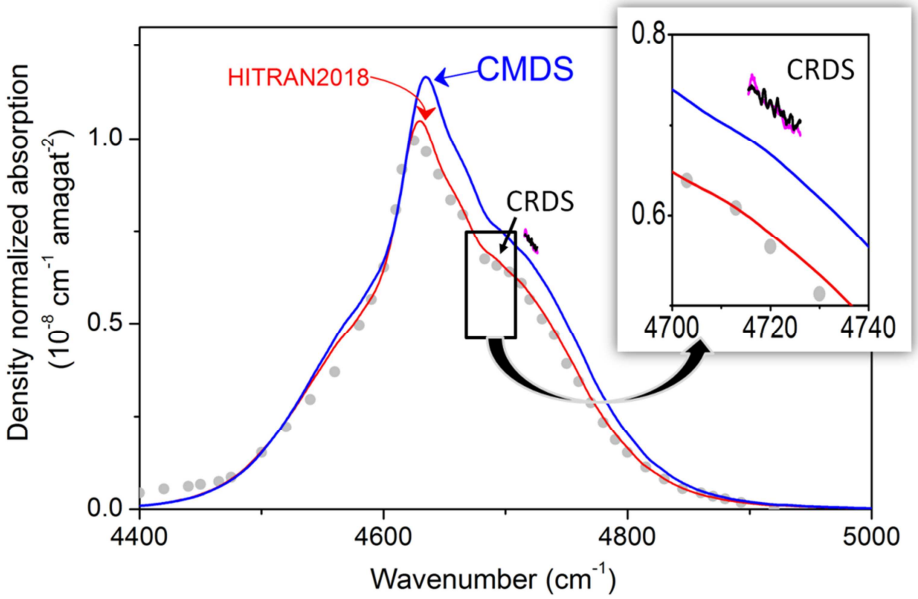

Fig. 5
Comparison between the room temperature $B_{N_2-N_2}$ binary coefficients of the 2-0 CIA band of N_2 obtained from CRDS recordings at 700 Torr (magenta) and 750 Torr (black) between 4715 and 4726 cm^{-1} to those *(i)* measured by Shapiro and Gush at high pressure (45-90 atm) [14] (grey dots) *(ii)* obtained by Hartmann *et al.* from classical molecular dynamics simulations (CMDS) (blue line) [13] and *(iii)* recommended by a recent update of the HITRAN database (red line) [10].

The same treatment is applied to the four N_2-O_2 spectra recorded at 750 Torr. The different Rayleigh cross-sections of Ar and air leads to a 5.4×10^{-11} cm^{-1} difference on the Rayleigh contribution to the extinction coefficient at 750 Torr. Taking into account this small contribution, the retrieved CIA of the N_2-O_2 mixture is the sum of two terms: $\alpha_{CIA}(\nu,T) = B_{N_2-N_2}(\nu,T)\rho_{N_2}^2 + B_{N_2-O_2}(\nu,T)\rho_{N_2}\rho_{O_2}$. After subtraction of the self-CIA contribution using our experimental determination of $B_{N_2-N_2}$ (**Table 2**), the $B_{N_2-O_2}(\nu,T)$ coefficient was determined by division by $\rho_{N_2}\rho_{O_2}$. The $B_{N_2-O_2}(\nu,T)$ values retrieved from the four recorded spectra are presented in **Fig. 6** together with a linear fit of their frequency dependence. In spite of the dispersion of the measured values, a clear decrease is evidenced over the 10 cm^{-1} spectral interval of the recordings. The N_2-O_2 contribution to the measured N_2 CIA is on the order of the 20% relative abundance of O_2 in air. Thus the 3% error bar on $B_{N_2-N_2}$ has a large impact on the uncertainty of the retrieved $B_{N_2-O_2}$ values. Taking into account the baseline

uncertainty, the overall uncertainty on $B_{N_2-O_2}$ is estimated to be 1.4×10^{-9} cm^{-1} $amagat^{-2}$ (i.e. ~30 % relative error).

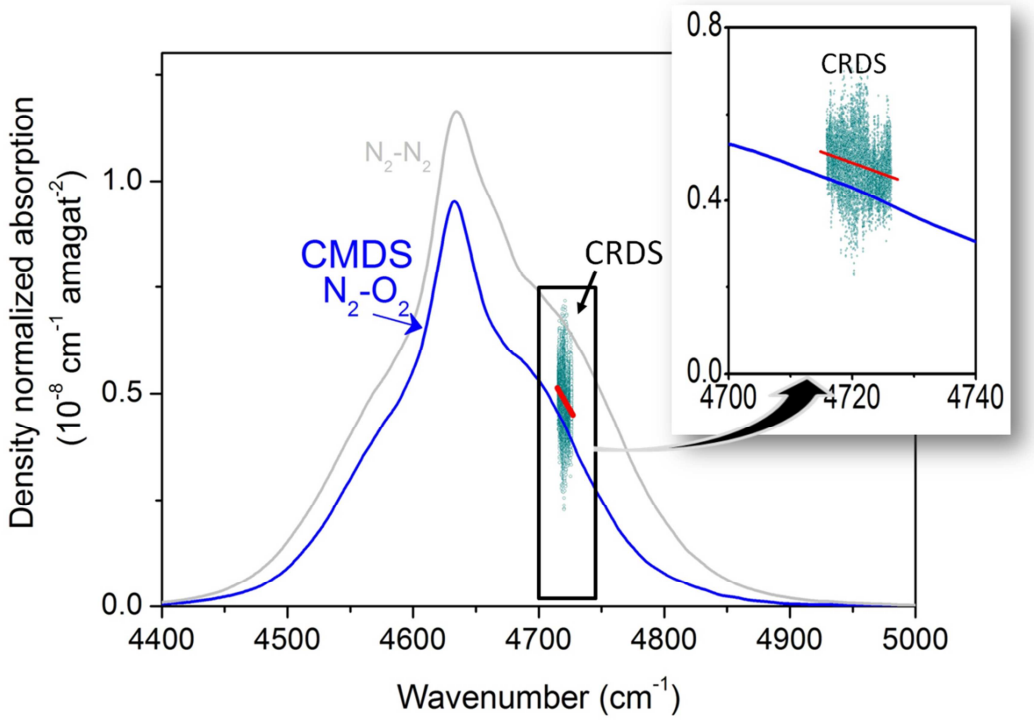

Fig. 6

Comparison of the room temperature $\boldsymbol{B_{N_2-O_2}}$ binary coefficients of the 2-0 CIA of N_2 obtained by classical molecular dynamics simulations (CMDS) (blue line) [13] to the CRDS measurements between 4715 and 4726 cm^{-1}. The cyan dots correspond to the measured spectra corrected from the contribution of the lines and of the N_2-N_2 CIA. The red segment corresponds to the linear fit of the measured values. The $\boldsymbol{B_{N_2-N_2}}$ binary coefficients as predicted by CMDS (grey line) are plotted for comparison.

3.2. Comparison to literature

We have gathered in **Fig. 5** the few literature results available for the 2-0 CIA of N_2. As indicated in **Table 1**, the only previous experimental investigation was performed in 1966 by Shapiro and Gush who used a high pressure cell associated with a grating spectrograph [14]. Pressure values as high as 90 atm were used, enhancing the CIA absorption by about four orders of magnitude compared to our sub-atmospheric measurements. Our CIA values reported with 3 % error bar are about 20 % higher than these pioneering results. Although this difference is not considerable, it exceeds by a factor of 2 the 10% error bar given by Shapiro and Gush on the integrated intensity of the 2-0 CIA band.

The results of classical molecular dynamics simulations (CMDS) recently performed by Hartmann et al. [13] are also included in **Fig. 5**. These calculations consider an ensemble of 10^6 N_2 molecules in interactions described by the force field taken from Ref. [32]. In this approach, the

absorption spectrum is obtained from a Fourier-Laplace transform of the auto-correlation function of the transition dipole moment. As illustrated in **Fig. 5**, a convincing agreement is achieved between CMDS results and measurements of Shapiro and Gush. In view of atmospheric applications, Hartmann et al. applied some corrections to their CMDS results in order to match the CIA measured by Shapiro and Gush at room temperature and by McKellar at 97.5 K [17]. A 5 cm^{-1} spectral shift and a linear function with temperature, $f(T) = 0.9 - 0.00125(296 - T)$, was applied, leading to a 10% decrease on the CDMS amplitude at 296 K. The empirically corrected CMDS CIA, very close to the results of Shapiro and Gush, is that recently recommended by the HITRAN database (see **Fig. 5**). We note that the application of the 0.9 empirical correction factor to the CMDS CIA leads to 20 % deviation between the HITRAN CIA and our CRDS results near 4720 cm^{-1} while the deviation with the original CMDS values was limited to 8 %.

In the case of the N_2-O_2 CIA, to our knowledge, no other experimental data are available for comparison. Our mean $B_{N_2-O_2}(v,T)$ coefficients show a clear decrease in the range of the studied spectral interval, in good agreement with the CMDS frequency dependence. Nevertheless, our values near 4720 cm^{-1} are larger by about 14 %. This deviation is similar to that obtained for the self-CIA but smaller than our estimated error bar on $B_{N_2-O_2}$. Note that, in agreement with our measurements, the $B_{N_2-N_2}$ self- coefficients predicted by CMDS are larger than the $B_{N_2-O_2}$ coefficients (see **Fig. 6**). At our measurement point, the $B_{N_2-N_2}/B_{N_2-O_2}$ ratio is about 1.59 and 1.43 for CMDS and CRDS, respectively.

4. The 2–0 *S*(10) and *S*(11) electric quadrupolar transitions

As illustrated in **Fig. 1**, the transitions of the 2-0 quadrupolar band of N_2 are extremely weak (maximum intensity around 6×10^{-30} cm/molecule). They are observed with a small S/N ratio in some of the FTS atmospheric spectra recorded at high zenith angle in the frame of the TCCON [7,13]. To our knowledge, the only laboratory detection of a 2-0 transition is that of the *O*(14) line by CRDS near 4518 cm^{-1} [11]. By combining a feedback narrowed DFB laser diode with a passive cell tracking technique, a limit of detection of $\alpha_{min} \sim 1.2\times10^{-11}$ cm^{-1} was achieved after one day of spectra averaging, allowing for the evaluation of the intensity of this line, on the order of 1.5×10^{-30} cm/molecule. In the present work, we used a similar approach to measure the 2–0 *S*(10) and *S*(11) transitions. Three series of spectra were recorded, at 100 Torr (68 spectra) and 200 Torr (194 spectra) around the *S*(10) transition and at 200 Torr (151 spectra) around the *S*(11) transition. About 16 minutes were needed to acquire each spectrum, about 2 cm^{-1} wide. In all cases, the spectra were recorded in flow regime to contain water vapor desorption from the cell over the long measurement period (up to 64 hours in total). The gas flow was regulated with a proportional electrovalve controlled by a software based-proportional-integral loop. The high finesse cell was filled with pure N_2 either from a tank (Air Liquide, 99.9999% purity) for the series of spectra at 200 Torr around the *S*(10) transition or from nitrogen evaporating of a liquid nitrogen tank in the case of the two other spectra series. The latter

nitrogen source was preferred for frequency calibration of the spectra as it contains higher water vapour concentration (~350 ppm compared to a few ppm) allowing for a better calibration of the spectra.

For each spectrum the minimum detectable absorption coefficient (corresponding to the baseline noise) was typically 1.2×10^{-10} cm^{-1}, mostly limited by interference fringes. The wavenumber scale of the spectrum, obtained from the wavelength meter (model 621-A IR from Bristol, 8 MHz accuracy), was refined by fitting water transitions in every single spectrum. The $5_{2\ 3}$-$6_{1\ 6}$ and $3_{0\ 3}$-$2_{1\ 2}$ transitions of the $3\nu_2$ band of $H_2{}^{16}O$ at 4716.7788 and 4725.4166 cm^{-1}, respectively, were selected as reference position for the calibration of the *S*(10) and *S*(11) spectra, respectively. The former is given in HITRAN 2016 with an uncertainty better than 1×10^{-4} cm^{-1} and an air pressure shift of -0.0018 cm^{-1} atm^{-1}. The position of the latter has a uncertainty of 1×10^{-3} cm^{-1} and a pressure shift of -0.0035 $cm^{-1}atm^{-1}$. For each recorded spectrum, the centers of the $H_2{}^{16}O$ and N_2 lines were determined using a multiline fit with a Voigt profile as line shape having Gaussian width fixed according to molecular mass and cell temperature. The differences between the HITRAN and fitted positions of the reference line, including pressure shift, were subsequently fitted against spectrum rank number - i.e. relative to time - by a second order polynomial smoothing the noisy and slow wavemeter calibration drift. This polynomial was used to recalibrate the individual spectra. To improve the signal to noise, the calibrated spectra series was then averaged. The procedure consisted in binning data points falling within a determined slice of the spectrum. The mean wavenumber and mean absorption coefficient were computed for every spectral bin. Bin widths of 2×10^{-3} cm^{-1} were adopted. In an individual spectrum, the number of ring down measurements corresponding to a given spectral bin was around 50. As a result, for example, each bin of the averaged spectrum around the *S*(11) transition corresponds to the statistical averaging of about 7500 ring down measurements. **Figs. 7 and 8** illustrate the gain achieved by averaging. Minimum detectable absorption coefficients, α_{min}, down to 8×10^{-12} cm^{-1} and 1.1×10^{-11} cm^{-1} were achieved around the *S*(10) and *S*(11) lines at 200 Torr, leading to signal to noise ratios of 110 and 40, respectively.

Positions and intensities of the *S*(10) and *S*(11) transitions, retrieved from a multiline fit of the final calibrated and averaged spectra, are reported in **Table 3**. The line profile fit of the *S*(10) line at 200 Torr is included in **Fig. 7.**

The uncertainties on the fitted positions, reported in **Table 3,** are mainly due to the very large uncertainty on the pressure shifts (±0.01 cm^{-1} atm^{-1}) provided in the HITRAN database for the two water reference lines. Note that for the *S*(10) 2-0 transition for which spectra recorded at 100 Torr and 200 Torr are at our disposal, the extrapolation at zero pressure of the position difference between N_2 and water reference line centers is not affected by the uncertainty on the pressure shifts (see Ref. [11]). The *S*(10) 2-0 line center extrapolated at zero pressure is given as a note of **Table 3.** Finally, as a validation of the obtained calibration, let us mention that the water lines near 4716.131 cm^{-1} and 4717.474 cm^{-1} located near the *S*(10) transition (**Fig. 7**), have their fitted positions within 0.001 cm^{-1}

from the HITRAN positions (known at ±0.001 cm^{-1}) even though they were not used for calibration of the spectra.

During the recording of a series of spectra, the temperature can vary over 0.8 K, nevertheless the impact on the intensity is limited due to the very low sensitivity of these N_2 lines to the temperature: 0.02% and 0.09% per Kelvin for the *S*(10) and *S*(11) line, respectively. Even if pressure is stabilized, fluctuations on the order of 0.6% are observed during the tens of hours of the recordings, impacting the intensity determination at the same level. Taking into account the signal to noise ratios, uncertainties on the integrated intensities are estimated to be in the 6-10 % range for the two transitions depending of the pressure (see **Table 3**).

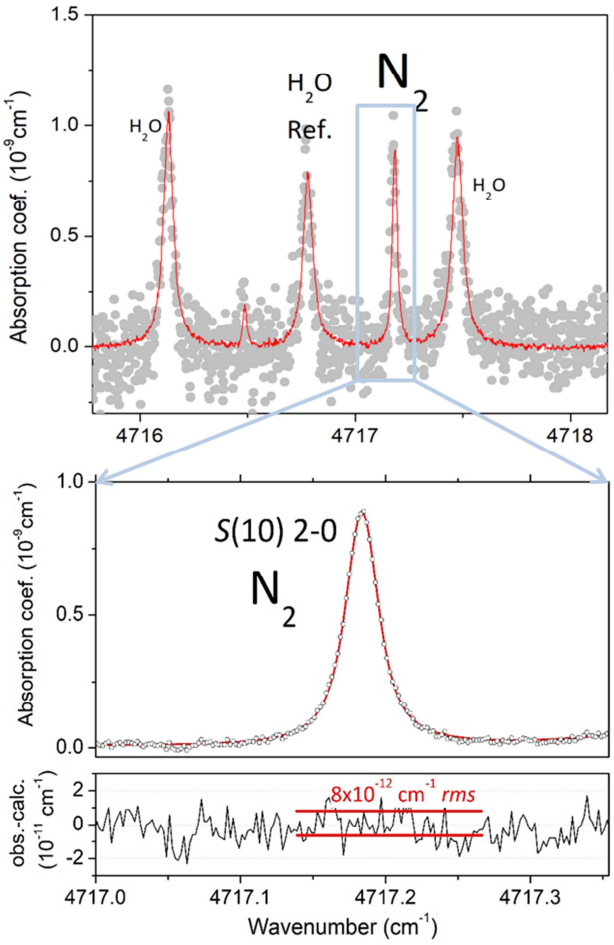

Fig. 7.

Spectra around the *S*(10) 2-0 transition of N_2 recorded at 200 Torr.

Upper panel: An example of an individual spectrum (grey circles) and spectrum obtained by averaging 194 such individual spectra (solid red). The CRDS measurement points were gathered within 2×10^{-3} cm^{-1} wide bins (see Text). The line at 4716.7788 cm^{-1} due to water (present as an impurity) was used as reference for the frequency calibration of the CRDS spectra.

Lower panel: Line profile fit of the N_2 line using a Voigt profile. The residuals of the fit reach the noise level corresponding to a minimum detectable absorption of 8×10^{-12} cm^{-1}.

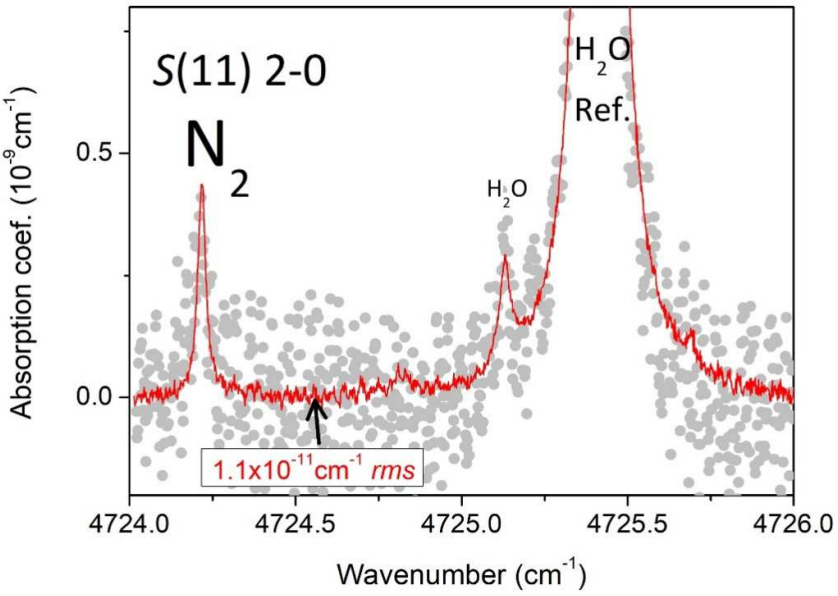

Fig. 8.

Spectra around the *S*(11) 2-0 transition of N_2 averaged from 151 single spectra with 2×10^{-3} cm^{-1} bins. The $H_2{}^{16}O$ line near 4725.4166 cm^{-1} ($3_{0\ 3}$-$2_{1\ 2}$ of the $3\nu_2$ band) was used as reference for the absolute calibration of the frequency axis. A minimum detectable absorption of 1.1×10^{-11} cm^{-1} is achieved for the averaged spectrum.

Table 3.

Positions and intensities derived for transitions of the (2-0) band of N_2 and comparison to HITRAN2016.

Transition	Pressure (Torr)	Position (cm^{-1})		Line intensity (cm/molecule)	
		Meas.	HITRAN2016 [b]	Meas.	HITRAN2016
O(14) 2-0		4518.4115±0.0030 [23]	4518.4128 ±0.01	1.26×10^{-30}±20% [23]	1.405×10^{-30}±20%
S(10) 2-0	100	4717.1866±0.0014 [a]	4717.1882 ±0.01	5.55×10^{-30}±10%	6.02×10^{-30}±20%
	200	4717.1869±0.0027 [a]		5.57×10^{-30}±6%	
S(11) 2-0	200	4724.2177±0.0036	4724.2218±0.01	3.03×10^{-30}±10%	2.71×10^{-30}±20%

Note.

[a] Extrapolation at zero pressure gives a value of 4717.1866(10) cm^{-1} (see Text).

[b] Zero-pressure values. No air pressure-shift on the line position is provised in the HITRAN database [10]

Compared to HITRAN values, the *S*(10) and *S*(11) line positions differ by -1.5×10^{-3} cm^{-1} and -0.9×10^{-3} cm^{-1}, respectively. A similar shift of -1.3×10^{-3} cm^{-1} was reported in Ref. [23] for the *O*(14) transition. The HITRAN line positions were derived from the semi-empirical potential energy function of Le Roy et al. [33]. The observed shifts are largely within the error bars of the line positions given in HITRAN (0.01 cm^{-1}). Our (scarce) dataset seems to evidence a systematic shift on the order of 1×10^{-3} cm^{-1}, close to our accuracy on the line center determinations. HITRAN intensities of the N_2 electric quadrupolar lines were derived from the *ab initio* quadrupole moment function of Li and Le Roy [34]

and are given in HITRAN with a 20% uncertainty. Compared to HITRAN values, the CRDS intensities show relative differences of -7.5%, +12.0%, -10% for the *S*(10), *S*(11) and *O*(14) transitions, respectively. No regular trend is observed for the three measured transitions, indicating that these deviations have probably an experimental origin and that the theoretical intensities are fully validated by the present measurements.

5. Concluding remarks

On the basis of highly sensitivity spectra recorded by OF-CEAS and CRDS, literature data about the collision induced absorption (CIA) and very weak electric quadrupolar transitions have been tested at two spectral points of the fundamental and first overtone bands of nitrogen. Although very limited in terms of spectral coverage, these new data are found to be valuable:

(i) The considered CIA measurements were performed for the first time at sub-atmospheric pressure allowing to check the agreement with previous high pressure measurements up to 8 atm [12,14,16] and 90 atm [14] for the 1-0 and 2-0 bands, respectively. The pure quadratic dependence of the CIA amplitude was carefully checked during pressure ramps up to 1 atm and from series of spectra recorded at different pressures, for the 1-0 and 2-0 measurement points, respectively.

(ii) A good agreement with the results of Lafferty et al. [16] and Baranov et al. [12] are obtained for the 1-0 band. In the case of the 2-0 CIA band, our CRDS determination near 4720 cm^{-1} exceeds by 20% the high pressure value of Shapiro and Gush [14]. Our CIA binary coefficients retrieved at 4720 cm^{-1} are supported by an agreement at the 3% level for determinations from CRDS spectra recorded at 700 and 750 Torr. The CMDS 2-0 CIA calculated by Hartmann et al. [13] was empirically adjusted to the high pressure measurements while they were originally closer to our value (difference of about 8%).

(iii) Although being extremely weak (line intensity on the order of a few 10^{-30} cm/molecule), the position and intensity of the 2–0 *S*(10) and *S*(11) electric quadrupolar transitions could be measured for the first time. Although more accurate, the obtained values fully validate the theoretical line list provided by the HITRAN database on the basis of Refs. [33,34]. A systematic shift on the line position on the order of 1×10^{-3} cm^{-1} is tentatively evidenced.

The present study performed by OF-CEAS and CRDS has provided a further illustration of the performances of these two highly sensitive cavity enhanced techniques. While a high sensitivity is required to detect the very weak quadrupolar electric transitions of N_2, the baseline stability is the main criterion for reliable measurements of the CIA.

Acknowledgements

This project is supported by the Labex OSUG@2020 (ANR10 LABX56), the LEFE-ChAt program from CNRS -INSU and the Breath- Diag project (ANR-15-CE18-0 0 06-01). The authors thank K. Jaulin (AP2E company) for lending us the 4 μm ICL laser. We would like to thank JM Hartmann (LMD, Paris) for providing us the original data of classical molecular dynamics simulations (CMDS) relative to the N_2-O_2 CIA presented in Ref. [13].

References

[1] Goldman A, Reid J, Rothman LS. Identification of electric quadrupole O_2 and N_2 lines in the infrared atmospheric absorption spectrum due to the vibration-rotation fundamentals. Geophys Res Lett 1981;8(1):77-78. https://doi.org/10.1029/GL008i001p00077.

[2] Camy-Peyret C, Flaud J-M, Delbouille L, Roland G, Brault JW, Testerman L. Quadrupole transitions of the 1<-0 band of N_2 observed in a high resolution atmospheric spectrum. J Phys Lett 1981; 42(13):L279-L283.

[3] Reuter D, Jennings DE, Brault JW. The n = 1 <- 0 quadrupole spectrum of N_2. J Mol Spectrosc 1986;115(2):294-304. https://doi.org/10.1016/0022-2852(86)90048-2.

[4] Rinsland P, Zander R, Goldman A, Murcray FJ, Murcray DG, Gunson MR, Farmer CB. The fundamental quadrupole band of $^{14}N_2$: Line positions from high-resolution stratospheric solar absorption spectra. J Mol Spectrosc 1991;148(1):274-279. https://doi.org/10.1016/0022-2852(91)90055-F.

[5] Kassi S, Gordon IE, Campargue A. First detection of transitions in the second quadrupole overtone band of nitrogen near 1.44 μm by CW-CRDS with 6×10^{-13}cm^{-1} sensitivity. Chem Phys Lett 2013;582:6-9. https://doi.org/10.1016/j.cplett.2013.07.031.

[6] Li H, Le Roy RJ. Quadrupole moment function and absolute infrared quadrupolar intensities for N_2. J Chem Phys 2007;126(22):224301. https://doi.org/10.1063/1.2739524.

[7] Total Carbon Column Observing Network, http://www.tccon.caltech.edu/; 2018 [accessed 13 December 2018]

[8] Frommhold L. Collision-Induced Absorption in Gases. Cambridge Univ Press; 1994. https://doi.org/10.1017/CBO9780511524523.

[9] Gordon IE, Rothman LS, Hill C, Kochanov RV, Tan Y, Bernath PF, Birk M, Boudon V, Campargue A, Chance KV, Drouin BJ, Flaud J-M, Gamache RR, Hodges JT, Jacquemart D, Perevalov VI, Perrin A, Shine KP, Smith M-AH, Tennyson J, Toon GC, Tran H, Tyuterev VG, Barbe A, Csaszar AG, Devi VM, Furtenbacher T, Harrison JJ, Hartmann J-M, Jolly A, Johnson TJ, Karman T, Kleiner I, Kyuberis AA, Loos J, Lyulin OM, Massie ST, Mikhailenko SN, Moazzen-Ahmadi N, Müller HSP, Naumenko OV, Nikitin AV, Polyansky OL, Rey M, Rotger M, Sharpe SW, Sung K, Starikova E, Tashkun SA, Vander Auwera J, Wagner G, Wilzewski J, Wcisło P, Yu S, Zak EJ. The HITRAN2016 molecular spectroscopic database. J Quant Spectrosc Radiat Transf 2017;203:3-69. https://doi.org/10.1016/j.jqsrt.2017.06.038.

[10] Richard C, Gordon IE, Rothman LS, Abel M, Frommhold L, Gustafsson M, Hartmann J-M, Hermans C, Lafferty WJ, Orton GS, Smith KM, Tran H. New section of the HITRAN database: Collision-induced absorption (CIA). J Quant Spectrosc Radiat Transf 2012;113(11):1276-1285. https://doi.org/10.1016/j.jqsrt.2011.11.004.

[11] Čermák P, Vasilchenko S, Mondelain D, Kassi S, Campargue A. First detection of an absorption line of the first overtone electric quadrupolar band of N_2 by CRDS near 2.2μm. Chemical Physics Letters 2017; 668:90–94. https://doi.org/10.1016/j.cplett.2016.11.002.

[12] Baranov Y, Lafferty W, Fraser G. Investigation of collisioninduced absorption in the vibrational fundamental bands of O_2 and N_2 at elevated temperatures. J Mol Spectrosc 2005;233(1):160-163. https://doi.org/10.1016/j.jms.2005.06.008.

[13] Hartmann J-M, Boulet C, Toon GC. Collision-induced absorption by N_2 near 2.16 μm: Calculations, model, and consequences for atmospheric remote sensing. J Geophys Res: Atmos 2017;122:2419-2428. https://doi.org/10.1002/2016JD025677.

[14] Shapiro MM, Gush HP. The collision-induced fundamental and first overtone bands of oxygen and nitrogen. Can J Phys 1966;44(5):949–963. https://doi.org/10.1139/p66-079.

[15] Menoux V, Doucen RL, Boulet C, Roblin A, Bouchardy AM. Collision-induced absorption in the fundamental band of N2: temperature dependence of the absorption for N_2-N_2 and N_2-O_2 pairs. Applied optics 1993;32(3):263-268. https://doi.org/10.1364/AO.32.000263.

[16] Lafferty WJ, Solodov AM, Weber A, Olson WB, Hartmann J-M. Infrared collision-induced absorption by N_2 near 4.3 μm for atmospheric applications: measurements and empirical modeling. Applied Optics 1996;35(30):5911-5917. https://doi.org/10.1364/AO.35.005911.

[17] McKellar ARW. Low-temperature infrared absorption of gaseous N_2 and $N_2 + H_2$ in the 2.0–2.5 μm region: Application to the atmospheres of Titan and Triton. Icarus 1989;80(2):361–369. https://doi.org/10.1016/0019-1035(89)90146-2.

[18] Ventrillard I, Romanini D, Mondelain D, Campargue A. Accurate measurements and temperature dependence of the water vapor self-continuum absorption in the 2.1 μm atmospheric window. J Chem Phy 2015;143(13):134304. https://doi.org/10.1063/1.4931811.

[19] Campargue A, Kassi S, Mondelain D, Vasilchenko S, Romanini D. Accurate laboratory determination of the near infrared water vapor self-continuum: A test of the MT_CKD model. J Geophys Res Atmos 2016;121:13,180–13,203. https://doi.org/10.1002/2016JD025531.

[20] Richard L, Vasilchenko S, Mondelain D, Ventrillard I, Romanini D, Campargue A. Water vapor self-continuum absorption measurements in the 4.0 and 2.1 μm transparency windows. J Quant Spectrosc Rad Transf 2017;201:171–179. http://doi.org/10.1016/j.jqsrt.2017.06.037.

[21] Lechevallier L, Vasilchenko S, Grilli R, Mondelain D, Romanini D, Campargue A. The water vapour self-continuum absorption in the infrared atmospheric windows: new laser measurements near 3.3 and 2.0 μm. Atmos Meas Tech 2018;11(4):2159–2171. https://doi.org/10.5194/amt-11-2159-2018.

[22] Mondelain D, Kassi S, Campargue A. Accurate laboratory measurement of the O_2 collision□induced absorption band near 1.27 μm. J Geophys Res: Atmos 2018;123. https://doi.org/10.1029/2018JD029317.

[23] Morville J, Romanini D, Kachanov AA, Chenevier M. Two schemes for trace detection using cavity ringdown spectroscopy. Appl Phys B 2004;78:465–476. https://doi.org/10.1007/s00340-003-1363-8.

[24] Morville J, Romanini D, Kerstel E. Cavity Enhanced Absorption Spectroscopy with Optical Feedback. In: Cavity-Enhanced Spectroscopy and Sensing. Springer; 2014, p163-209. https://doi.org/10.1007/978-3-642-40003-2_5.

[25] Sioris CE, Boone CD, Nassar R, Sutton KJ, Gordon IE, Walker KA, Bernath PF. Retrieval of carbon dioxide vertical proles from solar occultation observations and associated error budgets for ACE-FTS and CASS-FTS. Atmospheric Meas Tech 2014;7:2243-2262. https://doi.org/10.5194/amt-7-2243-2014.

[26] Romanini D, Kachanov AA, Sadeghi N, Stoeckel F. CW cavity ring down spectroscopy. Chem Phys Lett 1997;264(3-4):316–322. https://doi.org/10.1016/S0009-2614(96)01351-6.

[27] Kassi S, Campargue A. Cavity ring-down spectroscopy with 5×10^{-13} cm^{-1} sensitivity. J Chem Phys 2012;137(23):234201. https://doi.org/10.1063/1.4769974.

[28] Mondelain D, Vasilchenko S, Cermak P, Kassi S, Campargue A. The self- and foreign-absorption continua of water vapor by cavity ring-down spectroscopy near 2.35 μm. Phys Chem Chem Phys 2015;17:17762. DOI:10.1039/C5CP01238D

[29] Cermák P, Chomet B, Ferrieres L, Vasilchenko S, Mondelain D, Kassi S, et al. CRDS with a VECSEL for broad-band high sensitivity spectroscopy in the 2.3 μm window. Rev Sci Instrum 2016;87(8):083109. doi: 10.1063/1.4960769.

[30] Lin Q, Van Camp MA, Zhang H, Jelenkovic´ B,Vuletic´ B. Long-external-cavity distributed Bragg reflector laser with sub-kilohertz intrinsic linewidth. Opt Lett 2012;37,1989. https://doi.org/10.1364/OL.37.001989

[31] Thalman R, Zarzana K, Tolbert MA, Volkamer R. Rayleigh scattering cross-section measurements of nitrogen, argon, oxygen and air. J Quant Spectrosc Radiat Transfer 2014;147:171–177. https://doi.org/10.1016/j.jqsrt.2014.05.030.

[32] Bouanich J. Site-site Lennard-Jones potential parameters for N_2, O_2, H_2, CO and CO_2. J Quant Spectrosc Radiat Transfer 1992;47(4):243-250. https://doi.org/10.1016/0022-4073(92)90142-Q

[33] Le Roy RJ, Huang Y, Jary C. An accurate analytic potential function for ground-state N_2 from a direct-potential-fit analysis of spectroscopic data. J Chem Phys 2006;125, 164310. https://doi.org/10.1063/1.2354502

[34] Li H, Le Roy RJ. Quadrupole moment function and absolute infrared quadrupolar intensities for N_2. J Chem Phys 2007;126,224301. https://doi.org/10.1063/1.2739524

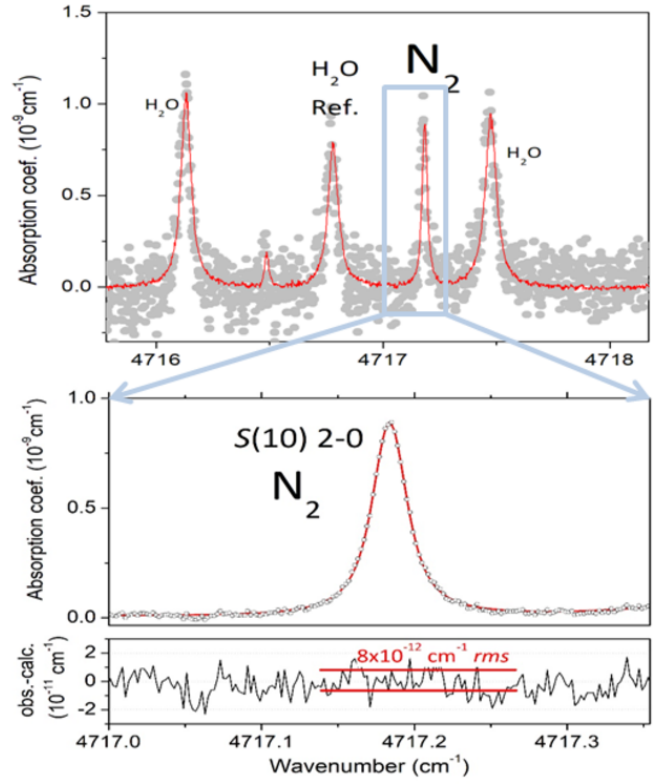
H2O
Ref.
N2
H2O
H2O
Absorption coef. (10-9cm-1)
4716
4717
4718
S(10) 2-0
N2
8x10-12 cm-1 rms
obs.-calc. (10-11 cm-1)
4717.0
4717.1
4717.2
4717.3
Wavenumber (cm-1)

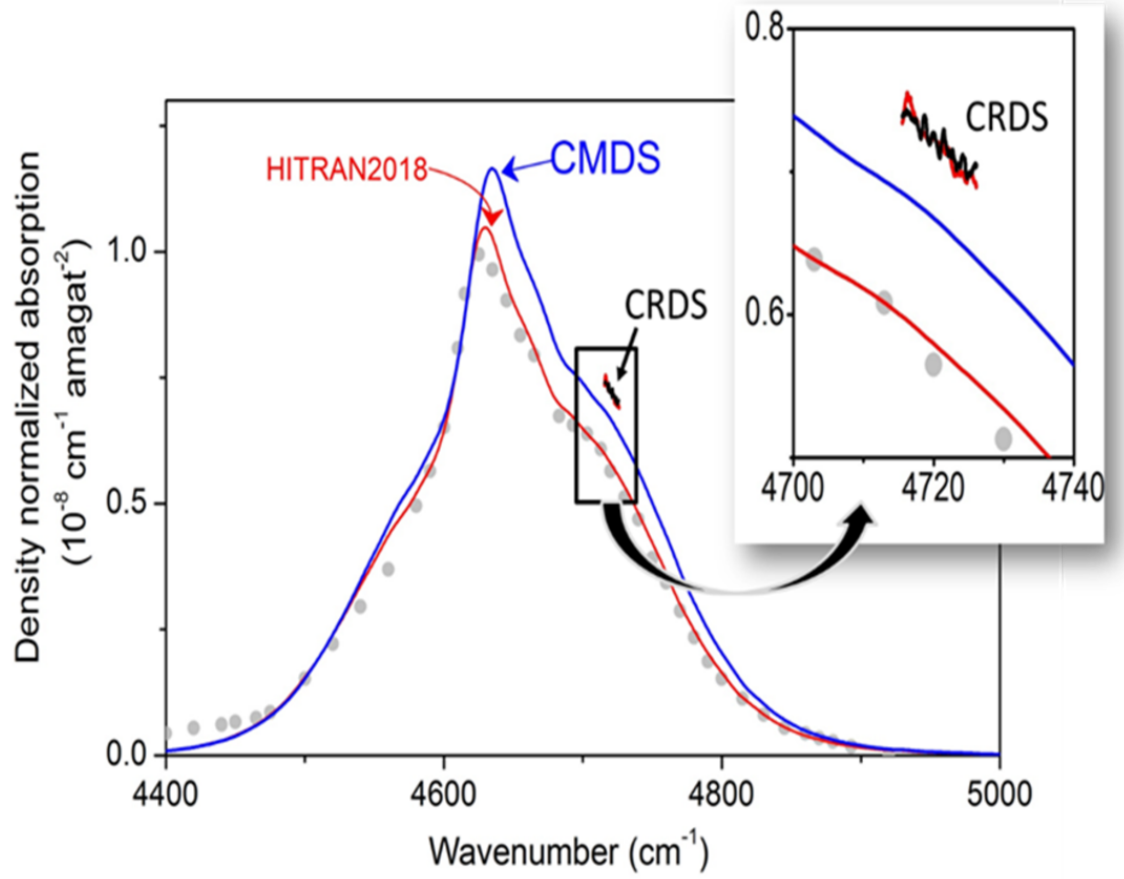
HITRAN2018
CMDS
CRDS
CRDS
Density normalized absorption (10-8 cm-1 amagat-2)
4400
4600
4800
5000
Wavenumber (cm-1)
4700
4720
4740